Photoinduced Microsecond-Charge-Separation in Retinyl-C_{60} Dyad

Mariko Yamazaki, Yasuyuki Araki,† Mamoru Fujitsuka,* and Osamu Ito*

Institute of Multidisciplinary Research for Advanced Materials, Tohoku University, Katahira, Aoba-ku, Sendai, 980-8577, Japan

Received: February 12, 2001; In Final Form: June 27, 2001

Intramolecular photoinduced charge separation and recombination processes in a retinyl-C_{60} dyad molecule (Ret-C_{60}) have been investigated in various solvents by time-resolved absorption and fluorescence techniques. Upon laser excitation of the C_{60}-moiety in nonpolar toluene, the intersystem crossing proceeded from the excited singlet state of the C_{60}-moiety (Ret-$^1C_{60}$*) to the excited triplet state (Ret-$^3C_{60}$*), followed by energy transfer yielding the excited triplet state of the retinyl-moiety (^{3}Ret*-C_{60}) without charge separation. On the other hand, in polar solvents such as *N*,*N*-dimethylformamide and benzonitrile, the charge separation occurred from Ret-$^1C_{60}$* at rate on the order of 10^{10} s^{-1}. The quantum yield was close to unity in these polar solvents. Most parts of the ion pair (Ret$^{\bullet+}$-$C_{60}^{\bullet-}$) changed to Ret-$^3C_{60}$* and ^{3}Ret*-C_{60} by the charge recombination which took place at rate on the order of 10^9 s^{-1}. However, some parts of the charge-separated state were kept in microsecond time-region: The lifetimes of Ret$^{\bullet+}$-$C_{60}^{\bullet-}$ were 16 μs and 19 μs in DMF and benzonitrile, respectively, which were as long as those of Ret-$^3C_{60}$* and ^{3}Ret*-C_{60}, suggesting an equilibrium between the charge-separated state and the excited triplet states.

Introduction

Intramolecular photoinduced energy and/or electron-transfer processes in donor−acceptor linked molecules have attracted considerable interests in the studies of the light-energy conversion system. Recently, fullerene-donor dyads have been studied by several groups due to their unique photophysical and photochemical properties.[1−8] Since C_{60} has a low reduction potential (−0.51 V vs SCE, in benzonitrile),[9] it acts as a good electron acceptor in the dyads. Various fullerene-donor dyads have been synthesized. As for donors of the dyad molecules, amine compounds,[2] carotenoid,[3] porphyrin,[4] ferrocene,[5] tetrathiafulvalene,[6] oligothiophene,[7] and so on[8] have been employed. The lifetimes of the charge-separated states were usually as short as a few nanoseconds.[2−8]

Clarifications of the roles of retinyl polyenes in the visual and photosynthetic systems have been one of the important research subjects in the spectroscopic and photochemical studies.[10] Nowadays, various retinyl polyenes with reactive functional groups are commercially available. Thus, these are useful reagents to synthesize new compounds. Furthermore, in the view of transient absorption spectroscopy, the intense and sharp absorption band of the radical cation of retinyl polyene is a good spectral probe in the visible region.[11a] In the mixture system of C_{60} and retinol, it has been confirmed that the electron-transfer took place via the excited triplet state of C_{60} ($^3C_{60}$*) as well as the energy transfer.[11a] In the case of β-carotene, which has a similar polyene backbone to retinyl compounds, it has been employed as the donor moiety of the dyads frequently. The photoinduced charge separation (CS) processes of carotenoid-C_{60} dyad have been investigated.[3] In this dyad molecule, the quantum yield of the CS process via the singlet-excited C_{60}-moiety ($^1C_{60}$*) was close to unity. From these results, it is expected that retinyl polyene is one of the candidates for the donor of the dyad.

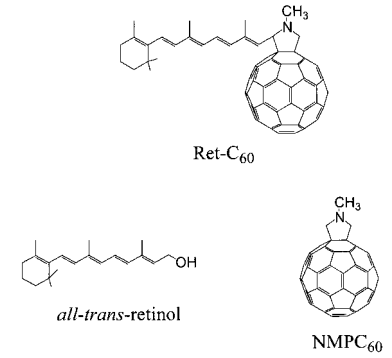

Figure 1. Molecular structures of Ret-C_{60}, $NMPC_{60}$, and *all-trans* retinol.

In the present study, we have investigated the photoinduced CS process in a covalently linked retinyl-C_{60} dyad (Figure 1) by the transient absorption spectroscopy. In addition, we took the time-resolved fluorescence measurements. Upon excitation of the C_{60}-moiety, the CS process occurred from the excited singlet state of the C_{60}-moiety in polar solvents. About two-thirds of the ion pair decayed within a few nanoseconds, however, the remaining one-third was kept in the microsecond time region. An equilibrium between the CS state and the excited triplet states was proposed for the CS state in the microsecond region.

Experimental Section

Materials. C_{60} was obtained from Term USA (purity = 99.9%). Other chemicals and solvents were of best grade commercially available.

Synthesis of Fullerene Derivatives. *N*-Methylpyrrolidinofullerene ($NMPC_{60}$) was obtained with the procedure described in the literature.[1c]

* To whom correspondence should be addressed.

† Institute of Multidisciplinary Research for Advanced Materials, Tohoku University, CREST, Japan Science and Technology Corporation (JST), Katahira, Aoba-ku, Sendai, 980-8577, Japan.

10.1021/jp0105490 CCC: $20.00
Published on Web 08/30/2001

Retinyl-Linked Fullerene (Ret-C_{60}).[1c] A mixture of *N*-methylglycine (62.1 mg, 0.67 mmol), *all-trans*-retinal (10.0 mg, 0.035 mmol), and C_{60} (40.8 mg, 0.054 mmol) in toluene (35 mL) was refluxed under a nitrogen atmosphere in the dark for 2 h; then the solvent was evaporated under vacuum. The reaction mixture was purified by column chromatography (silica gel, benzene/*n*-hexane = 20:1). Recrystallization from benzene-MeOH gave Ret-C_{60} as brown solid (27.7 mg, 0.027 mmol, 77.1%). ^{1}H NMR (400 MHz, $CDCl_3$) δ 1.00 (s, 6H, $-CH_3$), 1.47 (t, 2H, $-CH_2-$), 1.56 (m, 2H, $-CH_2-$), 1.69 (s, 3H, $-CH_3$), 1.96 (s, 3H, $-CH_3$), 2.00 (t, 2H, $-CH_{2-}$), 2.15 (s, 3H, $-CH_3$), 2.85 (s, 3H, N$-CH_3$), 4.15 (d, 1H, pyrrolidine$-$H), 4.86 (m, 2H, pyrrolidine$-$H), 6.02 (d, 1H, =CH$-$), 6.13 (m, 3H, =CH$-$), 6.56 (m, 2H, =CH$-$); ^{13}C NMR (100 MHz, $CDCl_3$) δ 12.84, 14.12, 19.23, 21.74, 28.95, 33.04, 34.23, 39.56, 40.25, 69.71, 69.79, 76.56, 77.56, 125.83, 127.16, 129.44, 129.78, 129.83, 135.74, 136.09, 136.97, 137.62, 137.83, 140.13, 140.77, 142.06, 142.11, 142.19, 142.59, 142.68, 143.13, 144.41, 144.67, 145.33, 145.42, 145.46, 145.53, 145.85, 145.96, 146.20, 146.34, 147.11, 147.30, 147.32, 153.64, 154.15, 156.12, 157.23; MALDI-TOF-MS *m*/*z* 1030.89 ($M^{\bullet+}$); Redox potentials of Ret-C_{60} were 0.95 V ($Ret^{\bullet+}$/Ret) and -0.55 V ($C_{60}/C_{60}^{\bullet-}$) vs Ag/AgCl in benzonitrile.

Apparatus. The picosecond laser flash photolysis was carried out using a second harmonic generation (SHG, 532 nm) of an active/passive mode-locked Nd:YAG laser (Continuum, PY61C-10, 35 ps fwhm) as an excitation source. The excitation laser pulse was depolarized. A streak camera (Hamamatsu Photonics, C2830) was employed as a detector in the measurements of the transient absorption spectra up to 5 ns. The breakdown of Xe gas was used as a probe light of the streak camera system as described previously.[11b] For the measurements of the transient absorption spectra in the visible and near-IR regions, the pump$-$probe system with a dual MOS detector (Hamamatsu Photonics, C6140) was applied. The time resolution of the present system was ca. 35 ps.[2f,7b,c]

Nanosecond transient absorption measurements were carried out using SHG (532 nm) or third harmonic generation (THG, 355 nm) of a Nd:YAG laser (Spectra-Physics, Quanta-Ray GCR-130, 6 ns fwhm) as an excitation source. For transient absorption spectra in the near-IR region (600$-$1200 nm), monitoring light from a pulsed Xe-lamp was detected with a Ge-APD detector. For spectra in the visible region (400$-$1000 nm), a photomultiplier or a Si$-$PIN photodiode was used as a detector. Details of the transient absorption measurements were described in our previous papers.[11] All the samples in a quartz cell (1 $\times$ 1 cm) were deaerated by bubbling Ar through the solution for 10 min.

The time-resolved fluorescence spectra were measured by a single-photon counting method using a SHG (410 nm) of a Ti:sapphire laser (Spectra-Physics, Tsunami 3950-L2S, 1.5 ps fwhm) and a streakscope (Hamamatsu Photonics, C43334$-$01) equipped with a polychromator.[2f,7b,c]

Steady-state absorption spectra in the visible and near-IR regions were measured on a spectrophotometer (Jasco V570 DS). Steady-state fluorescence spectra were measured on a spectrofluorophotometer (Shimadzu RF-5300 PC).

^{1}H and ^{13}C NMR spectra were recorded on a JEOL Lambda 400 spectrometer. Time-of-light mass spectrum was measured on a MALDI-TOF-MS instrument (Bruker REFLEX III-T) using α-cyano-4-hydroxycinnamic acid as a matrix. Cyclic voltammetry was carried out using a potentiostat (Hokuto Denko, HAB-151) in a conventional three-electrode cell equipped with Pt working and counter electrodes and an Ag/AgCl reference electrode at room temperature.

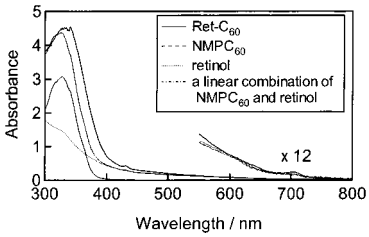

Figure 2. Absorption spectra of Ret-C_{60}, $NMPC_{60}$, *all-trans* retinol, and a linear combination of the spectra of $NMPC_{60}$ and *all-trans* retinol in DMF (path length; 1 cm).

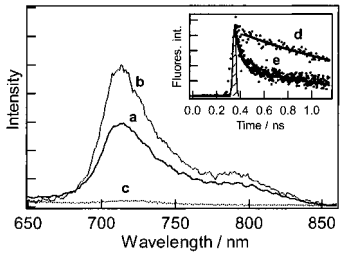

Figure 3. Fluorescence spectra of (a) Ret-C_{60} (0.07 mM), (b) $NMPC_{60}$ (0.11 mM) in toluene, and (c) Ret-C_{60} (0.06 mM) in DMF; excitation at 410 nm. Inset: Fluorescence-time profiles around 720 nm of Ret-C_{60} in (d) toluene and (e) DMF. Solid lines show fitted curves. Hatched part indicates laser profile.

Results and Discussion

Steady-State Absorption Spectra. Figure 2 shows an absorption spectrum of Ret-C_{60} in *N*,*N*-dimethylformamide (DMF) as well as those of $NMPC_{60}$, *all-trans* retinol and a linear combination of $NMPC_{60}$ and retinol. The absorption band of the dyad around 332 nm is shifted to a longer wavelength and becomes broad relative to that of the linear combination of $NMPC_{60}$ and retinol. These small spectral changes indicate weak interactions between the components of the dyad. In the present laser photolysis studies, the 532- or 355-nm laser light was employed as the excitation source. The 532-nm laser light predominantly excites the C_{60}-moiety of the dyad. On the other hand, the 355-nm laser light is absorbed by the retinyl- and C_{60}-moieties at the ratio of ca. 50:50.

Steady-State Fluorescence Spectra. Figure 3 shows fluorescence spectra of Ret-C_{60} and $NMPC_{60}$. In toluene, the fluorescence spectrum-a resulting from the C_{60}-moiety of Ret-C_{60}, is quite similar with the spectrum-b of $NMPC_{60}$. Quantitative analyses on the fluorescence properties were carried out based on the lifetime measurements. From the fluorescence-decay profile of Ret-C_{60} around 720 nm (time profile-d in inset of Figure 3), the fluorescence lifetime (τ_F) of the excited singlet state of the C_{60}-moiety (Ret-$^1C_{60}$*) in nonpolar toluene was estimated to be 1.3 ns, which is the same as $NMPC_{60}$ (τ_F = 1.3 ns).[12] The finding excludes the possibility of energy transfer from Ret-$^1C_{60}$* to the excited singlet state of the retinyl-moiety (^{1}Ret*-C_{60}), which is reasonable because the singlet energy of the retinyl group (3.33 eV)[13] is higher than that of C_{60} (1.74 eV).[14] Therefore, it can be concluded that the intersystem crossing from Ret-$^1C_{60}$* to the excited triplet state of the C_{60}-moiety (Ret-$^3C_{60}$*) occurred in nonpolar solvent (eq 1).

$$\text{Ret-}C_{60} \xrightarrow[\textit{in non-polar solvent}]{h\nu\ (532\ \text{nm})} \text{Ret-}{}^1C_{60}^{*} \xrightarrow{k_{ISC}} \text{Ret-}{}^3C_{60}^{*} \quad (1)$$

In DMF, the fluorescence band resulting from the C_{60}-moiety was completely quenched in the steady-state measurement (spectrum-c). The fluorescence decay profile in DMF (time profile-e in inset of Figure 3) can be analyzed by two decay

TABLE 1: Free Energy Changes for Charge Separation ($-\Delta G_{CS}$), Fluorescence Lifetimes (τ_F), Singlet Quenching Rates (k_q^S), Quantum Yields for Charge Separation (Φ_{CS}), and Rates of First Charge Recombination Step (k_{CS}^I) of Ret-C_{60} in Various Solvents

compound	solvent[a]	ϵ_{solv}[b]	$-\Delta G_{CS}$/eV[c]	τ_F/s	k_q^S/s^{-1}	Φ_{CS}	k_{CR}^I/s^{-1}[d]
Ret-C_{60}	DMF	36.71	0.30	7.3×10^{-11}	1.3×10^{10}	0.94	6.8×10^{9}
	BN	25.2	0.29	8.1×10^{-11}	1.2×10^{10}	0.94	2.6×10^{9}
	THF	7.58	0.19	9.8×10^{-11}	9.4×10^{9}	0.92	3.1×10^{9}
	ANS	4.38	0.10	6.3×10^{-10}	9.0×10^{8}	0.54	2.2×10^{8}
	Tol	2.38	−0.11	1.3×10^{-9}	−[e]	–	–
$NMPC_{60}$[f]	Bz	2.28	–	1.3×10^{-9}	–	–	–

[a] DMF, *N*,*N*-dimethylformamide; BN, benzonitrile; THF, tetrahydrofuran; ANS, anisole; Tol, toluene; Bz, benzene. [b] Data from ref 13. [c] $-\Delta G_{CS} = \Delta E_{0-0} - (-\Delta G_{CR})$, $-\Delta G_{CR} = E_{ox} - E_{red} + \Delta G_S$, $\Delta G_S = e^2/(4\pi\epsilon_0)[(1/(2R^+)+1/(2R^-) - 1/R_{cc})(1/\epsilon_s) - (1/(2R^+) + 1/(2R^-))(1/\epsilon_r)]$, where ΔE_{0-0} is energy of the 0−0 transition of C_{60}; E_{ox} and E_{red} are first oxidation potential of the donor and the first reduction potential of the acceptor in benzonitrile, respectively; R^+ and R^- are radii of the ion radicals of retinyl (8.2 Å) and C_{60} (4.7 Å), respectively; R_{cc} is center-to-center distance between the two moieties (11.4 Å); ϵ_s and ϵ_r are static dielectric constants of solvents used for the rate measurements and the redox potential measurements. [d] The k_{CS}^I value was estimated by applying first-order decay function to the quick decay of the $Ret^{\bullet+}$-moiety, which was observed in the picosecond laser flash photolysis. [e] The CS process was not observed. [f] Data from ref 12.

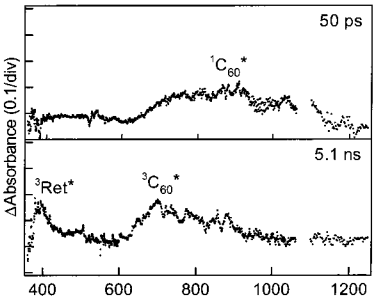

Figure 4. Picosecond transient absorption spectra of Ret-C_{60} (0.20 mM) in toluene at 50 ps and 5.1 ns after 532-nm laser irradiation.

components; a slow-decaying part is a minor component (ca. 20%), compared with a fast-decaying component (ca. 80%). Although such decay with two components was observed in DMF, benzonitrile, and tetrahydrofuran (THF), one component decay was observed in less polar solvents such as anisole and toluene. From the time-resolved fluorescence spectra, both components can be attributed to the fluorescence from the C_{60}-moiety. Lifetimes of the initial main component are summarized in Table 1. The data shows that the fluorescence lifetimes of Ret-$^1C_{60}$* become shorter with increasing solvent polarity. Thus, a new quenching pathway, including the CS process in the dyad, participates in the deactivation process of Ret-$^1C_{60}$* in these polar solvents. Quenching rates of the singlet state (k_q^S) were estimated as summarized in Table 1 from the relation, $k_q^S = (\tau_F)^{-1} - (\tau_0)^{-1}$, where τ_0 is the fluorescence lifetime of $NMPC_{60}$ in benzene.

As for the slow-decaying component, contribution of the charge recombination (CR) or other pathway is expected as mentioned in the next section.

Picosecond Laser Flash Photolysis. To obtain more detailed information on the photoinduced processes of Ret-$^1C_{60}$*, transient absorption spectra in the picosecond region were measured. Figure 4 shows transient absorption spectra of Ret-C_{60} in toluene obtained by the 532-nm laser light irradiation which excites the C_{60}-moiety. The broad absorption band around 900 nm, which appeared immediately after the laser irradiation, is attributed to the absorption band of Ret-$^1C_{60}$* from the similarity with an $S_n \leftarrow S_1$ absorption band of C_{60}.[15] At 5.1 ns after the laser, absorption spectrum showed bands around 400 and 710 nm, of which the latter is characteristic to Ret-$^3C_{60}$*.[12] The band around 400 nm corresponds to the excited triplet state of the retinyl-moiety (^{3}Ret*-C_{60}),[16] which seems to overlap with the absorption bands of Ret-$^3C_{60}$*. The transient absorption bands resulting from the CS state were not observed. These findings indicate that the intersystem crossing process occurred

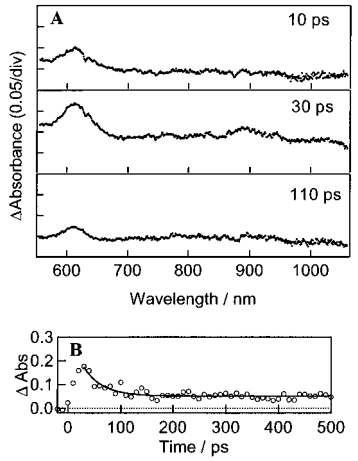

Figure 5. (A) Picosecond transient absorption spectra of Ret-C_{60} (0.34 mM) in DMF at 10, 30, and 110 ps after 532-nm laser irradiation. (B) Absorption−time profile at 610 nm.

without the CS process in nonpolar toluene, as expected from the steady-state and the time-resolved fluorescence measurements. Since the 532-nm laser light predominantly excites the C_{60}-moiety of the dyad, ^{3}Ret*-C_{60} is considered to be generated by energy transfer from Ret-$^3C_{60}$*, which is reasonable process because the triplet energy level of retinyl polyene is lower than C_{60}.[11a]

As for Ret-C_{60} in DMF, transient absorption bands were observed around 610 and 900 nm immediately after the laser irradiation (Figure 5A). These bands can be attributed to the radical cation of the retinyl-moiety ($Ret^{\bullet+}$).[10,11a] An absorption band resulting from the radical anion of the C_{60}-moiety ($C_{60}^{\bullet-}$), which would be anticipated to appear around 1000 nm,[12] seems to overlap with the absorption band resulting from the $Ret^{\bullet+}$-moiety around 900 nm. These findings indicate that $Ret^{\bullet+}$-$C_{60}^{\bullet-}$ is formed by the CS process from Ret-$^1C_{60}$* (eq 2). Similar CS process was also observed in benzonitrile and THF.

$$\text{Ret-}C_{60} \xrightarrow[\textit{in polar solvents}]{h\nu\ (532\ \text{nm})} \text{Ret-}{}^1C_{60}^{*} \xrightarrow[\Phi_{CS}]{k_{CS}} \text{Ret}^{\bullet+}\text{-}C_{60}^{\bullet-} \qquad (2)$$

The CS process from Ret-$^1C_{60}$* was also confirmed by the subpicosecond laser photolysis experiments in benzonitrile (See Supporting Information, Figure 1S); from absorption−time profile at 610 nm, the generation rate of the radical cation was estimated to be 1.5×10^{10} s^{-1}, which corresponded well with the decay rate of fluorescence of $^1C_{60}$*-moiety (1.2×10^{10} s^{-1}). These findings support the CS process as eq 2. In Table 1, the k_q^S values were estimated from the time-resolved fluorescence measurements. As mentioned in above section, the k_{CS} value

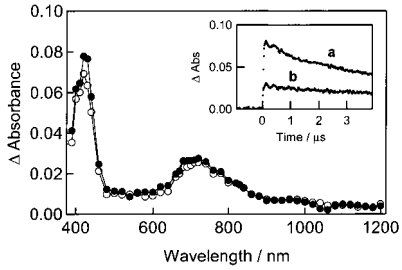

Figure 6. Nanosecond transient absorption spectra of Ret-C_{60} (0.05 mM) in toluene at 100 ns (●) and 1.0 μs (○) after 532 nm-laser irradiation. Inset: Absorption−time profiles at (a) 430 nm and (b) 710 nm.

($=k_q^S$) increased with increasing solvent polarity (Table 1). The quantum yield for CS (Φ_{CS}) can be calculated from the relation, $\Phi_{CS} = k_{CS}/(k_{CS} + k_0) = ((\tau_F)^{-1} - (\tau_0)^{-1})/((\tau_F)^{-1})$, where k_0 is the fluorescence decay rate of $NMPC_{60}$. Although the Φ_{CS} values can be also obtained from the fluorescence intensity, we employed the value estimated from the fluorescence lifetime measurements in the present study, since comparison of fluorescence intensity does not give reliable values due to the fluorescence decay with two-components of the C_{60}-moiety. The Φ_{CS} values are also increased with an increase of solvent polarity as summarized in Table 1. The estimated Φ_{CS} values are as high as 0.94 in DMF and benzonitrile. The Φ_{CS} values close to unity indicate the efficient CS process of the dyad molecule with short donor−acceptor linkage in polar solvents. The Φ_{CS} values close to unity have been reported for various dyads including fullerene such as zincporphyrin-C_{60} and carotenoid-C_{60},[2−8] indicating high potential for application in light-harvesting system or solar cell.

As show in the time profile of Figure 5B, the concentration of the generated radical ions reached a maximum at ca. 30 ps after the laser irradiation, and then it decreased quickly until 200 ps down to ca. one-third. However, the absorption of the $Ret^{\bullet+}$-moiety did not decrease completely; ca. one-third of the $Ret^{\bullet+}$-moiety remained at 500 ps. As shown in the latter section, this remaining part was also observed in the microsecond time region. The quick decay of the absorption bands of the radical-ion pair can be attributed to the CR process in the dyad. By applying the first-order decay function to the quick-decay part, the rate for CR (k_{CR}^I), in which suffix I refers to the first CR step, was estimated to be 6.8×10^9 s^{-1} in DMF. The k_{CR}^I values estimated for the other reaction media are listed in Table 1, which increased with an increase in the solvent polarity, i.e., dielectric constant (ϵ_{solv}).

The CR process seems to regenerate Ret-$^1C_{60}$*, partly which may be observed as a slow-decaying part of the fluorescence-time profile (time profile-e in inset of Figure 3). Regeneration of the $^1C_{60}$*-moiety by CR of the charge-separated state is also reported for zincporphyrin-C_{60} dyad.[4] In fluorescence decay profiles, the slow-decaying parts become minor as solvent polarity increases. This finding accords with the fact that the CS state becomes more stable in more polar solvent. That is, the energy barrier from the CS state to Ret-$^1C_{60}$* increases in polar solvents.

Nanosecond Laser Flash Photolysis. From the results of the picosecond laser photolysis in nonpolar solvent, the deactivation process of Ret-$^1C_{60}$* was attributed to the intersystem crossing to Ret-$^3C_{60}$*. To confirm the processes in longer time scale, transient absorption measurements were carried out by the nanosecond laser photolysis using the 532-nm laser irradiation. Figure 6 shows transient absorption spectra of Ret-C_{60} in toluene. Two absorption bands of Ret-$^3C_{60}$* and ^{3}Ret*-C_{60} were

TABLE 2: Free Energy Changes for Charge Recombination ($-\Delta G_{CR}$), Rates for Second Charge Recombination Step (k_{CR}^{II}), Lifetimes of Radical-Ion Pair (τ_{IP}^{intra}), and Triplet Decay Rates ($k_T(C_{60})$ and k_T(Ret)) of Ret-C_{60} in Various Solvents

solvent[a]	$-\Delta G_{CR}$/ eV[b]	intramolecular			
		k_{CR}^{II}/s^{-1}	τ_{IP}^{intra}/s	$k_T(C_{60})/s^{-1}$	k_T(Ret)/s^{-1}
DMF	1.44	6.2×10^4[c]	1.6×10^{-5}[c]	5.5×10^4[c]	1.4×10^5[c]
BN	1.45	5.4×10^4[c]	1.9×10^{-5}[c]	4.8×10^4[c]	6.1×10^4[c]
Tol	1.85	—[d]	—[d]	1.0×10^5	1.8×10^5

[a] Abbreviation for solvents: See caption of Table 1. [b] The ΔG_{CR} values were estimated by the relation referred in the caption of Table 1. [c] The intramolecular k_{CR}^{II}, $k_T(C_{60})$, and k_T(Ret) values were evaluated from the intercepts of the pseudo-first-order plots (Figure 8B). Each experimental value contains estimation error of ±10%. [d] The CS process was not observed.

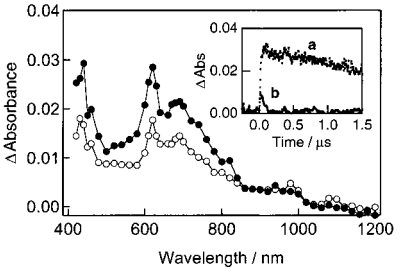

Figure 7. Nanosecond transient absorption spectra of Ret-C_{60} (0.21 mM) in DMF at 100 ns (●) and 1.0 μs (○) after 532 nm-laser irradiation. Inset: Absorption−time profiles at 610 nm in (a) the absence and (b) presence of oxygen.

clearly observed at 710 and 430 nm, respectively. This finding indicates that energy transfer occurred from a part of Ret-$^3C_{60}$* to ^{3}Ret*-C_{60} after the intersystem crossing from Ret-$^1C_{60}$* to Ret-$^3C_{60}$* as shown by the picosecond laser photolysis. The decay rate constants of Ret-$^3C_{60}$* ($k_T(C_{60})$) and ^{3}Ret*-C_{60} (k_T(Ret)) were estimated as summarized in Table 2. The $k_T(C_{60})$ value (1.0×10^5 s^{-1}) is slightly faster than the triplet decay rate constant of $NMPC_{60}$ in benzene (4.1×10^4 s^{-1}).[12] In toluene, relative quantum yields of triplet generation were evaluated from the maximal concentrations; for Ret-$^3C_{60}$*, $\Phi_{rel}(^3C_{60}^*) = [^3C_{60}^*]/\{[^3C_{60}^*] + [^3\text{Ret}^*]\} = 0.71$ and for ^{3}Ret*-C_{60}, $\Phi_{rel}(^3\text{Ret}^*) = [^3\text{Ret}^*]/\{[^3C_{60}^*] + [^3\text{Ret}^*]\} = 0.29$.

As for Ret-C_{60} in DMF, the picosecond-laser photolysis revealed that the photoinduced CS process occurred via Ret-$^1C_{60}$*, and then the absorption of $Ret^{\bullet+}$-$C_{60}^{\bullet-}$ decreased. However, the absorption band of the $Ret^{\bullet+}$-moiety still remained partly at 500 ps after laser pulse (Figure 5(B)). The long-lived $Ret^{\bullet+}$-moiety was confirmed by the nanosecond laser photolysis in DMF. In Figure 7, three transient-absorption bands were observed at 430, 610, and 710 nm. The absorption bands at 710 and 430 nm correspond to Ret-$^3C_{60}$* and ^{3}Ret*-C_{60}, respectively, and the absorption band at 610 nm can be attributed to the $Ret^{\bullet+}$-moiety. A weak absorption band was also observed around 980 nm, which can be attributed to another absorption band of the $Ret^{\bullet+}$- moiety overlapping with the absorption of the $C_{60}^{\bullet-}$-moiety. Ret-$^3C_{60}$* and ^{3}Ret*-C_{60} may be generated by the first CR step of $Ret^{\bullet+}$-$C_{60}^{\bullet-}$, because the quantum yield for CS from Ret-$^1C_{60}$* is almost unity in DMF. From the relative actinometry method using $^3C_{70}$* as an internal standard (for $^3C_{70}$*, $\epsilon = 6500$ M^{-1} cm^{-1} at 980 nm and $\Phi_{isc} = 0.9 \pm 0.15$)[17] and reported extinction coefficients of the excited triplet states of $NMPC_{60}$ ($\epsilon = 16\,100$ M^{-1} cm^{-1})[12] and retinol ($\epsilon = 57\,500$ M^{-1} cm^{-1}),[10] the quantum yields of Ret-$^3C_{60}$* formation and ^{3}Ret*-C_{60} formation were estimated to be 0.66 ± 0.15 and 0.10 ± 0.15, respectively. These findings indicate that the first CR

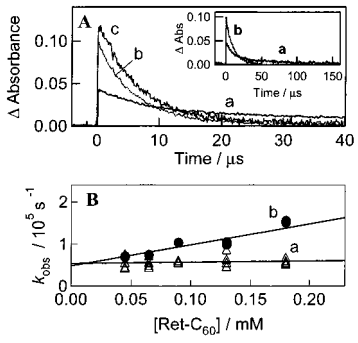

Figure 8. (A) Absorption−time profiles of Ret-C_{60} (0.18 mM) in benzonitrile at (a) 610 nm, (b) 710 nm and (c) 430 nm. Inset: Absorption−time profiles for long time scale. (B) Pseudo- first-order plots for (a) fast-decaying component of Ret$^{\bullet+}$-$C_{60}^{\bullet-}$ and (b) Ret-$^3C_{60}$* in benzonitrile.

step of Ret$^{\bullet+}$-$C_{60}^{\bullet-}$ generates the excited triplet states in high yields. That is, deactivation from Ret$^{\bullet+}$-$C_{60}^{\bullet-}$ to the ground state is minor process in the first CR step. The $\Phi_{rel}(^3C_{60}*)$ and $\Phi_{rel}(^3Ret*)$ values, immediately after laser pulse, were calculated to be 0.87 and 0.13, respectively. The $\Phi_{rel}(^3C_{60}*)$ value in polar solvent is higher than that in nonpolar solvent, which suggests that Ret-$^3C_{60}$* was generated efficiently from the first CR process in polar solvent. On the other hand, the absorption decay of Ret$^{\bullet+}$-$C_{60}^{\bullet-}$ observed in the nanosecond experiment can be attributed to the second CR step, which obeyed first-order kinetics. This second CR step deactivates to the ground state of the dyad. The rate constant of the second CR step (k_{CR}^{II}) was estimated to be 6.2×10^4 s^{-1}, which corresponds to 16 μs of the radical-ion pair lifetime. This value is much longer than the other donor-fullerene dyad molecules,[2−8] as discussed in the next section. Furthermore, the k_{CR}^{II} value did not show the dependence on the laser power and the concentration of the dyad.

It is worth mentioning that the absorption band of the Ret$^{\bullet+}$-moiety was quenched as well as those of Ret-$^3C_{60}$* and ^{3}Ret*-C_{60} in the presence of O_2 (time profile-b in inset of Figure 7). However, in the mixture system of NMPC_{60} and retinol, the absorption of the radical cation of retinol was not quenched by O_2, as shown in the later section. Furthermore, the electron-transfer rate of the radical anion of pristine C_{60} with O_2 was reported to be as slow as 3.7×10^2 M^{-1} s^{-1}.[18] Therefore, O_2 sensitivity of the radical ion in the present dyad suggests that the precursor of the radical-ion pair was quenched by O_2. Thus, it is presumed that the long-lived radical-ion pair observed in the microsecond time scale was produced from Ret-$^3C_{60}$* and ^{3}Ret*-C_{60}, and/or that the charge-separated state was in equilibrium with Ret-$^3C_{60}$* and ^{3}Ret*-C_{60}.

In benzonitrile, although similar CS and CR processes were observed, the decay of the Ret$^{\bullet+}$-moiety showed two components clearly (Figure 8(A)). Furthermore, the slower component in benzonitrile exhibited a considerable long lifetime of several hundred microseconds, while the absorptions of Ret-$^3C_{60}$* and ^{3}Ret*-C_{60} decayed completely within 40 μs (Figure 8A). In DMF, slow-decaying component could not be detected, probably due to very weak absorbance.

Concentration Effect. The decay rate constants of Ret-$^3C_{60}$* ($k_T(C_{60})$) and Ret$^{\bullet+}$-$C_{60}^{\bullet-}$ (k_{CR}^{II}) in benzonitrile were estimated as a function of the dyad concentration (Figure 8B). The $k_T(C_{60})$ values showed good linear correlation with the dyad concentration. Similar concentration dependence was also observed for the decay rate-constants of ^{3}Ret*-C_{60} (k_T(Ret)). These observations suggest that intermolecular electron transfer

TABLE 3: Lifetimes of Radical-Ion Pair (τ_{IP}^{intra}) of Various Dyads

donor−acceptor	solvent	τ_{IP}^{intra}/s	reference
phytochlorin−C_{60}	BN	7.0×10^{-11}	4g
carotenoid−C_{60}	CS_2	5.3×10^{-10}	3
porphyrin (H_2)−C_{60}	BN	4.5×10^{-8}	4j
BBA−C_{60}	BN	2.2×10^{-7}	2f
porphyrin (Zn)−C_{60}	BN	5.8×10^{-7}	4j
tetrathiophene−C_{60}	BN	6.3×10^{-6}	7b
retinyl−C_{60}	BN	2.0×10^{-5}	this study

occurred from Ret-$^3C_{60}$* and ^{3}Ret*-C_{60} to Ret-C_{60} in the ground state (eq 3), as reported for the tetrathiafulvalene-C_{60} dyad.[6]

$$\begin{matrix} \text{Ret–}^3C_{60}^* + \text{Ret–}C_{60} \\ {}^3\text{Ret}^*\text{–}C_{60} + \text{Ret–}C_{60} \end{matrix} \xrightarrow[k_{elt}^{inter}]{\text{intermolecular electron transfer}} \text{Ret}^{\cdot+}\text{–}C_{60} + \text{Ret–}C_{60}^{\cdot-} \quad (3)$$

As a result of the intermolecular electron transfer, the radical ions also showed long lifetime. From these findings, the fast- and slow-decaying components of the Ret$^{\bullet+}$-moiety can be attributed to the intra- and intermolecular CR processes, respectively.

The intermolecular electron-transfer rate constants, k_{elt}^{inter}-(via $^3C_{60}$*) and k_{elt}^{inter}(via ^{3}Ret*), were evaluated to be 5.0×10^8 M^{-1} s^{-1} and 4.4×10^8 M^{-1} s^{-1}, respectively, from the slopes of the pseudo-first-order plots. It is noteworthy that the lifetime of the radical ions generated by eq 3 was as long as 110 μs, when dyad concentration is 0.13 mM.

As for the intramolecular CR process, the k_{CR}^{II} value was independent of the dyad concentration as shown in Figure 8B, from which the intrinsic rate constants for the intramolecular processes such as k_{CR}^{II}, $k_T(C_{60})$ and k_T(Ret) values were evaluated as the intercepts (Table 2). The lifetime of the intramolecular ion pair (τ_{IP}^{intra}) was calculated to be 19 μs in benzonitrile from the reciprocal k_{CR}^{II} value. In DMF, the τ_{IP}^{intra} value was similarly evaluated to be 16 μs. In Table 3, the lifetimes of the ion pairs in some dyads including the C_{60}-moiety are summarized;[2−8] the reported values vary with the donor from $\tau_{IP}^{intra} = 70$ ps (phytochlorin-C_{60}) to $\tau_{IP}^{intra} = 6.3$ μs (tetrathiophene-C_{60}). Comparing with these reported values, the Ret-C_{60} dyad shows the longest τ_{IP}^{intra} value in the donor-C_{60} dyad systems.

Temperature Effect. To estimate the energy barrier for the second CR step experimentally, the k_{CR}^{II} values of Ret-C_{60} were measured as a function of temperature in DMF and benzonitrile. For benzonitrile, the fast-decaying component in the microsecond time scale was adopted for the analysis, since the slow-decaying component can be attributed to the intermolecular process as discussed above. The k_{CR}^{II} values were reduced with decreasing temperature in both solvents; i.e., the k_{CR}^{II} values in DMF were 3.5×10^5 s^{-1} at 307 K and 4.5×10^4 s^{-1} at 218 K. In benzonitrile, the k_{CR}^{II} values were 8.7×10^4 s^{-1} at 307 K and 3.2×10^4 s^{-1} at 264 K. On the other hand, the quantum yields for the CS process were scarcely influenced by temperature. From a semiclassical Marcus equation,[19] the electron-transfer rate constant (k_{elt}) can be described as follows (eq 4).

$$\ln(k_{elt}T^{1/2}) = \ln\{2\pi^{3/2}|V|^2/[h(\lambda k_B)^{1/2}]\} - \Delta G^{\ddagger}/(k_B T) \quad (4)$$

In eq 4, T is absolute temperature, $|V|$ is the electron coupling matrix element, h is the Planck constant, λ is the reorganization energy, k_B is the Boltzman constant, and $\Delta G^{\ddagger}$ is the Gibbs activation energy in Marcus theory.

Figure 9 shows modified Arrhenius plot,[2a,b,f,20] which shows a linear relation between $\ln(k_{CR}^{II}T^{1/2})$ values and $1/T$. The plots show no appreciable systematic deviation from the best-fit

TABLE 4: Experimental and Theoretical Activation Energies and Reorganization Energies for Ret−C_{60}

solvent [a]	$\Delta G_{CR}^{\ddagger}$(exp)/ eV[b]	$\Delta G_{CR}^{\ddagger}$(theor)/eV[c]	λ(exp)/eV[b]	λ(theor)/eV[c]	λ_s(theor)/eV[d]	$\|V\|$/cm^{-1} [b]	$\Delta G_{CS}^{\ddagger}$(theor)/eV[c]
DMF	0.133	0.144	0.80	0.78	0.48	0.44	0.071
BN	0.159	0.212	0.77	0.70	0.40	0.32	0.060

[a] Abbreviation for solvents: See caption of Table 1. [b] Determined experimentally from the modified Arrhenius plots (Figure 9). Estimation errors of $\Delta G_{CR}^{\ddagger}$ and $|V|$ values were ±4 and ±15%, respectively. [c] Determined theoretically. [d] The λ_s(theor) values were calculated from the relation,[21] $\lambda_s = e^2/(4\pi\epsilon_0)[(1/(2R^+) + 1/(2R^-) - 1/R_{cc})(1/n^2 - 1/\epsilon_s)]$, by employing the geometric parameters summarized in the footnote of Table 1; n is the index of refraction.

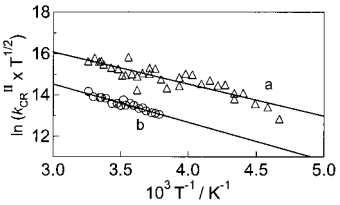

Figure 9. Modified Arrhenius plots (eq 4) of the temperature-dependent k_{CR}^{II} for Ret-C_{60} in (a) DMF and (b) benzonitrile.

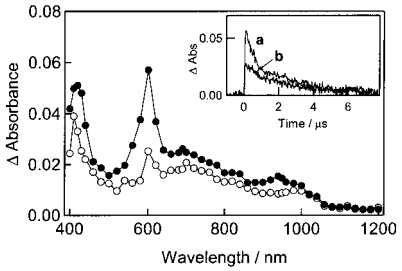

Figure 10. Nanosecond transient absorption spectra of Ret-C_{60} (0.05 mM) in DMF at 100 ns (●) and 1.0 μs (○) after 355-nm laser irradiation. Inset: Absorption−time profiles around (a) 610 nm and (b) 710 nm.

straight line. From the slope ($= -\Delta G_{CR}^{\ddagger}/k_B$), the $\Delta G_{CR}^{\ddagger}$(exp) values in DMF and benzonitrile were estimated to be 0.13 and 0.16 eV, respectively. The λ(exp) values were calculated from the relation, $\Delta G^{\ddagger} = (\Delta G_0 + \lambda)^2/(4\lambda)$ on putting $\Delta G_0 = \Delta G_{CR}$, and the $|V|$ values were estimated from the intercept ($=\ln\{2\pi^{3/2}|V|^2/[h(\lambda k_B)^{1/2}]\}$) as listed in Table 4.

The λ value can be divided into an internal term (λ_i), which originates from the internal molecular structural differences between the reactant and product, and a solvent term (λ_s), which is related to the differences of the orientation and polarization of solvent molecules between the initial and final states ($\lambda = \lambda_i + \lambda_s$). Here, when $\lambda_i = 0.3$ eV was employed as estimated by Williams et al. based on the charge-transfer absorption and emission of C_{60} and dimethylaniline,[2a,b] the λ_s(theor) values were evaluated as summarized in Table 4, by employing the geometric parameters listed in the footnote of Table 1. The λ_i and estimated λ_s(theor) values gave the λ(theor) values from the relation, λ(theor) $= \lambda_i + \lambda_s$(theor).[21] Using the λ(theor) and ΔG_0 ($=\Delta G_{CR}$) values, the $\Delta G_{CR}^{\ddagger}$(theor) values in DMF and benzonitrile were calculated to be 0.14 and 0.21 eV, respectively. These theoretical λ and $\Delta G_{CR}^{\ddagger}$ values are in considerably good agreement with the experimentally estimated values (Table 4). Since the $-\Delta G_{CR}$ values are larger than the λ(theor) values, the CR processes take place in the Marcus "inverted region".[19,20] An increase of the solvent polarity reduces the $-\Delta G_{CR}$ values; therefore, the k_{CR}^{II} value in DMF is larger than that in benzonitrile. Interestingly, the $|V|$ values are extremely small (0.44 and 0.32 cm^{-1} in DMF and benzonitrile, respectively) as compared to the reported values (1−100 cm^{-1}).[2−8] According to the Marcus theory,[19] the k_{elt} value is dominated by the $|V|$ value, the λ and ΔG_0 values associated with the electron-transfer process. Since the λ and ΔG_0 values in this study are almost the same as the reported values for the dyad systems, the small $|V|$ values may be one of the reasons for the observed slow k_{CR}^{II} values of Ret-C_{60} in polar solvents. Furthermore, the rate-limiting step of the second CR process will be the step deactivating to the ground state from Ret$^{\bullet+}$-$C_{60}^{\bullet-}$, since this step gives larger $\Delta G^{\ddagger}$ in the deactivation processes of Ret$^{\bullet+}$-$C_{60}^{\bullet-}$.

As for the first CR process, the process is considered to be in the Marcus "normal region", from the comparison of the λ value and free-energy change for the generation of triplet states from the CS state, which was the main deactivation process of the CS state in the picosecond region as discussed above.

In the case of the CS process, the $\Delta G_{CS}^{\ddagger}$(theor) values are estimated to be 0.07 and 0.06 eV in DMF and benzonitrile, respectively, by applying the λ(theor) and ΔG_0 ($=\Delta G_{CS}$) values to the relation, $\Delta G^{\ddagger} = (\Delta G_0 + \lambda)^2/(4\lambda)$. Williams et al. reported that the $\Delta G_{CS}^{\ddagger}$ value of dimethylaniline-C_{60} dyad is to be 0.11 eV in benzonitrile. Thus, smaller $\Delta G_{CS}^{\ddagger}$(theor) of Ret-C_{60} will be attributed to smaller λ(theor) of Ret-C_{60} (in benzonitrile, λ(theor) = 0.70 and 1.22 eV for Ret-C_{60} and dimethylaniline-C_{60}, respectively) due to larger size of the retinyl-moiety ($R^+ = 8.2$ Å) than the dimethylaniline-moiety ($R^+ = 3.7$ Å). From the comparison of the $-\Delta G_{CS}$ with λ(theor) values, the CS processes are assigned to the Marcus "normal region". Then, with the increase of the solvent polarity, the k_{CS} values increase due to the larger $-\Delta G_{CS}$ values.

Effect of Excitation Wavelength. In the above sections, all laser photolysis studies were carried out by the 532-nm laser light, which predominantly excited the C_{60}-moiety of the dyad. To learn more about the photoexcited properties of the Ret-C_{60} dyad, nanosecond laser photolysis experiment was carried out using the 355 nm-laser light, which excites both the retinyl- and C_{60}-moieties. As shown in Figure 10, the absorption band of the Ret$^{\bullet+}$-moiety around 610 nm became clear in DMF, when the dyad was excited by the 355-nm light. The finding indicates that CS occurred more efficiently than the CS process by the 532 nm-excitation. From the fluorescence lifetime measurements, it became clear that the rate and yield of the CS process from Ret-$^1C_{60}$* did not depend on the excitation wavelength. On the other hand, the $\Phi_{rel}(^3C_{60}*)$ and $\Phi_{rel}(^3Ret*)$ values were estimated to be 0.73 and 0.27, respectively, when the 355-nm laser was irradiated. The $\Phi_{rel}(^3Ret*)$ value is higher than that by the 532-nm light irradiation; $\Phi_{rel}(^3Ret*) = 0.15$ by the 532-nm laser. This finding can be attributed to the slow CS process from $^1Ret*$-C_{60}, since the CS from the $^1Ret*$-C_{60} is in the Marcus "inverted region". Actually, slow decay rate of $^1Ret*$-C_{60} was confirmed by the fluorescence decay measurement. The highly populated $^3Ret*$-C_{60} state shifts the equilibrium between $^3Ret*$-C_{60} and Ret$^{\bullet+}$-$C_{60}^{\bullet-}$ to the ion pair side. Thus, the absorption intensity of the Ret$^{\bullet+}$-moiety is considered to be increased as observed in Figure 10.

Mixture System of NMPC_{60} and Retinol. To confirm the O_2-insensitivity of the radical ions, transient absorption measurements were carried out in the mixture system of NMPC_{60} and *all-trans* retinol. Figure 11 shows the nanosecond transient absorption spectra obtained by the 532-nm laser irradiation of the mixture of NMPC_{60} (0.16 mM) and *all-trans*-retinol (12.4

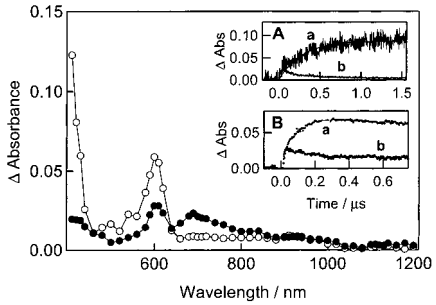

Figure 11. Nanosecond transient absorption spectra of $NMPC_{60}$ (0.16 mM) in the presence of *all-trans* retinol (12.4 mM) in DMF at 70 ns (●) and 1.0 μs (○) after 532 nm laser irradiation. Inset: (A) Absorption−time profiles at (a) 420 nm and (b) 700 nm. (B) Absorption−time profiles at 600 nm in (a) the absence and (b) presence of oxygen.

mM) in DMF. The transient absorption band of the excited triplet state of $NMPC_{60}$ ($^3NMPC_{60}$*) appeared at 700 nm immediately after the laser irradiation. With the decay of $^3NMPC_{60}$*, new absorption bands resulted from the triplet-excited retinol (^{3}Retinol*) and the radical cation of retinol (Retinol$^{\bullet+}$) appeared at 420 and 600 nm, respectively. In addition to these bands, two weak absorption bands were also observed around 940 and 1000 nm, which can be attributed to Retinol$^{\bullet+}$ and the radical anion of $NMPC_{60}$ ($NMPC_{60}^{\bullet-}$), respectively.[10,12] From these findings, it is clear that Retinol$^{\bullet+}$ and $NMPC_{60}^{\bullet-}$ were generated by the intermolecular electron-transfer process. Furthermore, the generation of ^{3}Retinol* by the energy transfer from $^3NMPC_{60}$* is also evident (eq 5). The quantum yields of the electron and energy transfer were estimated to be 0.60 and 0.40, respectively. These processes are reasonable from an energetic viewpoint, because the free energy changes of the electron and energy transfer were estimated to be −0.21 eV and −0.07 eV, respectively. The rate constants of the electron- and energy-transfers were estimated to be 3.9×10^8 M^{-1} s^{-1} and 2.6×10^8 M^{-1} s^{-1}, respectively. Both values are smaller than those values of the mixture system of pristine C_{60} and retinol.[11a]

$$^1NMPC_{60}^* \xrightarrow{k_{ISC}} {}^3NMPC_{60}^* \xrightarrow{\text{retinol}} \begin{cases} \xrightarrow{\text{electron-transfer}} NMPC_{60}^{\cdot-} + \text{Retinol}^{\cdot+} \\ \xrightarrow{\text{energy-transfer}} NMPC_{60} + {}^3\text{Retinol}^* \end{cases} \quad (5)$$

$$NMPC_{60} \xrightarrow{h\nu\ (532\text{nm})} {}^1NMPC_{60}^*$$

The contribution of $^1NMPC_{60}$* to both processes is negligibly small, because the fast intersystem crossing process from $^1NMPC_{60}$* to $^3NMPC_{60}$* is predominant deactivation process when the concentration of retinol is low (<50 mM).[22]

After reaching the maximum, the absorption intensity of Retinol$^{\bullet+}$ showed decay according to second-order kinetics due to the back electron transfer.

Although the absorption intensity of Retinol$^{\bullet+}$ decreased considerably in the presence of O_2, the decay rate of Retinol$^{\bullet+}$ was not accelerated comparing with that without O_2 (time profile-b in inset figure (B) of Figure 11). This finding indicates that Retinol$^{\bullet+}$ itself is insensitive to O_2. Electron transfer from $NMPC_{60}^{\bullet-}$ to O_2 is also a quite slow process.[18]

Energy Diagrams of the Dyad. Photoinduced processes of the present dyad molecule in nonpolar solvent (toluene) are summarized in the schematic energy diagram (Figure 12A). When the C_{60}-moiety was excited, the intersystem crossing from Ret-$^1C_{60}$* to Ret-$^3C_{60}$* occurred, and then energy transfer took place from Ret-$^3C_{60}$* to ^{3}Ret*-C_{60}. The CS from Ret-$^1C_{60}$* did not occur; because the energy level of the CS state is higher than that of Ret-$^1C_{60}$*.

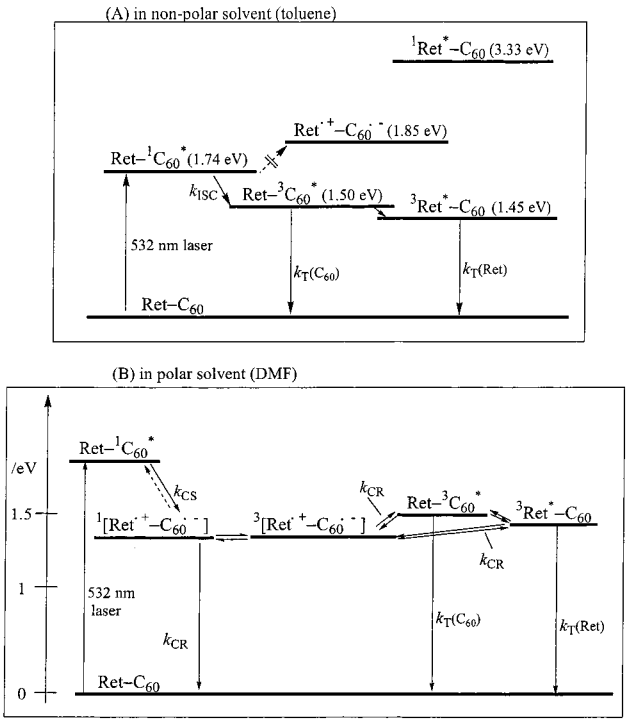

Figure 12. Schematic energy diagrams for energy- and electron-transfer processes in Ret-C_{60} dyad in (A) nonpolar (toluene) and (B) polar solvent (DMF). Numbers indicate energy levels in eV unit relative to the ground state.

In polar solvents, the CS process from Ret-$^1C_{60}$* took place immediately after the laser irradiation of the C_{60}-moiety (Figure 12B). Fast CS process can be attributed to the lower energy level of Ret$^{\bullet+}$-$C_{60}^{\bullet-}$. A small part of Ret$^{\bullet+}$-$C_{60}^{\bullet-}$ showed slow decay, which corresponds to 19 μs of lifetime in benzonitrile. The observed long lifetime of a radical ion pair can be attributed to the equilibrium with the triplet states, i.e., Ret-$^3C_{60}$* and ^{3}Ret*-C_{60}. These considerations seem to be adequate, since the energy levels of these triplet states locate quite closely to the CS state, as shown in Figure 12B. Thus, the energy levels of triplet states seem to be one of the important parameters in the molecular design necessary to achieve a long lifetime of the CS state.

Conclusion

In the present Ret-C_{60} dyad, photoinduced CS occurred immediately after the laser irradiation of the C_{60}-moiety in polar solvent, and the quantum yield of the ion pair formation was almost unity. After reaching a maximum at ≈30 ps, the absorption band of the Ret$^{\bullet+}$-moiety decayed as a result of the CR process, generating both Ret-$^3C_{60}$* and ^{3}Ret*-C_{60}. However, the absorption of the ion radical did not decrease completely. The radical-ion pair was also observed in the microsecond time region; the lifetime of radical-ion pair was as long as 19 μs in benzonitrile. This long lifetime of the radical-ion pair was led by the equilibrium between the CS state and the excited triplet states, since the energy levels of these three states locate closely in polar solvents. This equilibrium was supported by the sensitivity of the radical ion to O_2 in the present dyad.

Acknowledgment. The present work was partly supported by a Grant-in-Aid on Scientific Research from the Ministry of Education, Science, Sports and Culture of Japan (No. 12875163). The authors are also grateful to a financial support by Core Research for Evolutional Science and Technology (CREST) of

Japan Science and Technology Corporation. The authors also thank to The Kyozo Ogura Fund for Young Scientists.

Supporting Information Available: Transient absorption spectra of Ret-C_{60} in benzonitrile by subpicosecond laser excitation. This material is available free of charge via the Internet at http://pubs.acs.org.

References and Notes

(1) (a) Sun, Y.-P. In *Molecular and Supramolecular Photochemistry, Vol. 1, Organic Photochemistry;* Ramamurthy, V., Schanze, K. S., Eds.; Marcel Dekker: New York, 1977; pp 325−390. (b) Foote, C. S. In *Topics in Current Chemistry; Electron Transfer 1;* Matty, J., Ed.; Springer-Verlag: Berlin, 1994; p 347. (c) Maggini, M.; Scorrano, G.; Prato, M. *J. Am. Chem. Soc.* **1993**, *115*, 9798. (d) Kamat, P. V.; Asmus, K.-D. *Interface* **1996**, *5*, 22. (e) Imahori, H.; Sakata, Y. *Adv. Mater.* **1997**, *7*, 537. (f) Prato, M.; Maggini, M. *Acc. Chem. Res.* **1998**, *31*, 519. (g) Martin, N.; Sanchez, L.; Illescas, B.; Perez, I. *Chem. Rev.* **1998**, *98*, 2527.

(2) (a) Williams, R. M.; Zwier, M. N.; Verhoeven, J. W. *J. Am. Chem. Soc.* **1995**, *117*, 4093. (b) Williams, R. M.; Koeberg, M.; Lawson, J. M.; An, Y.-Z.; Rubin, Y.; Paddon-Row, M. N.; Verhoeven, J. W. *J. Org. Chem.* **1996**, *61*, 5055. (c) Thomas, K. G.; Biju, V.; George, M. V.; Guldi, D. M.; Kamat, P. V. *J. Phys. Chem. A* **1998**, *102*, 5341. (d) Thomas, K. G.; Biju, V.; Guldi, D. M.; Kamat, P. V.; George, M. V. *J. Phys. Chem. B* **1999**, *103*, 8864. (e) Thomas, K. G.; Biju, V.; Guldi, D. M.; Kamat, P. V.; George, M. V. *J. Phys. Chem. A* **1999**, *103*, 10755. (f) Komamine, S.; Fujitsuka, M.; Ito, O.; Moriwaki, K.; Miyata, T.; Ohno, T. *J. Phys. Chem. A* **2000**, *104*, 11497.

(3) Imahori, H.; Cardoso, S.; Tatman, D.; Lin, S.; Noss, L.; Seely, G. R.; Sereno, L.; Silber, C.; Moore, T. A.; Moore, A. L.; Gust, D. *Photochem. Photobiol.* **1995**, *62*, 1009.

(4) (a) Liddell, P. A.; Sumida, J. P.; Macpherson, A. N.; Noss, L.; Seely, G. R.; Clark, K. N.; Moore, A. L.; Moore, T. A.; Gust. D. *Photochem. Photobiol.* **1994**, *60*, 537. (b) Imahori, H.; Hagiwara, K.; Aoki, M.; Akiyama, T.; Taniguchi, S.; Okada, T.; Shirakawa, M.; Sakata, Y. *J. Am. Chem. Soc.* **1996**, *118*, 11771. (c) Imahori, H.; Hagiwara, K.; Akiyama, T.; Aoki, M.; Taniguchi, S.; Okada, T.; Shirakawa, M.; Sakata, Y. *Chem. Phys. Lett.* **1996**, *263*, 545. (d) Kuciauskas, D.; Lin, S.; Seely, G. R.; Moore, A. L.; Moore, T. A.; Gust, D.; Drovetskaya, T.; Reed, C. A.; Boyd, P. D. W. *J. Phys. Chem.* **1996**, *100*, 15926. (e) Gust, D.; Moore, T. A.; Moore, A. L. *Res. Chem. Intermed.* **1997**, *23*, 621. (f) Imahori, H.; Ozawa, S.; Uchida, K.; Takahashi, M.; Azuma, T.; Ajavakom, A.; Akiyama, T.; Hasegawa, M.; Taniguchi, S.; Okada, T.; Sakata, Y. *Bull. Chem. Soc. Jpn.* **1999**, *72*, 485. (g) Tkachenko, N. V.; Rantala, L.; Tauber, A. Y.; Helaja, J.; Hynninen, P. V.; Lemmetyinen, H. *J. Am. Chem. Soc.* **1999**, *121*, 9378. (h) Schuster, D. I.; Cheng, P.; Wilson, S. R.; Prokhorenko, V.; Katterle, M.; Holzwarth, A. R.; Braslavsky, S. E.; Klihm, G.; Williams, R. M.; Luo, C. *J. Am. Chem. Soc.* **1999**, *121*, 11599. (i) Imahori, H.; Sakata, Y. *Eur. J. Org. Chem.* **1999**, *2445*, 5. (j) Luo, C.; Guldi, D. M.; Imahori, H.; Tamaki, K.; Sakata, Y. *J. Am. Chem. Soc.* **2000**, *122*, 6535. (k) Imahori, H.; El-Khouly, M. E.; Fujitsuka, M.; Ito, O.; Sakata, Y.; Fukuzumi, S. *J. Phys. Chem. A* **2001**, *105*, 325.

(5) Guldi, D. M.; Maggini, M.; Scorrano, G.; Prato, M. *J. Am. Chem. Soc.* **1997**, *119*, 974.

(6) (a) Llacay, J.; Veciana, J.; Vidal-Gancedo, J.; Bourdelnde, J. L.; Gonzalez-Moreno, R.; Rovia, C. *J. Org. Chem.* **1998**, *63*, 5201. (b) Martin, N.; Sanchez, L.; Herranz, M. A.; Guldi, D. M. *J. Phys. Chem. A* **2000**, *104*, 4648.

(7) (a) Yamashiro, T.; Aso, Y.; Otsubo, T.; Tang, H.; Harima, T.; Yamashita, K. *Chem. Lett.* **1999**, 443. (b) Fujitsuka, M.; Ito, O.; Yamashiro, T.; Aso, Y.; Otsubo, T. *J. Phys. Chem. A* **2000**, *104*, 4876. (c) Fujitsuka, M.; Matsumoto, K.; Ito, O.; Yamashiro, T.; Aso, Y.; Otsubo, T. *Res. Chem. Intermed.* **2001**, *27*, 73. (d) Hirayama, D.; Yamashiro, T.; Takiyama, K.; Aso, Y.; Otsubo, T.; Norieda, H.; Imahori, H.; Sakata, Y. *Chem. Lett.* **2000**, 570. (e) van Hal, P. A.; Knol, J.; Langeveld-Voss, B. M. W.; Meskers, S. C. J.; Hummelen, J. C.; Janssen, R. A. J. *J. Phys. Chem. A* **2000**, *104*, 5974.

(8) (a) Sariciftci, N. S.; Wudl, F.; Heeger, A. J.; Maggini, M.; Scorrano, G.; Prato, M.; Bourassa, J.; Ford, P. C. *Chem. Phys. Lett.* **1995**, *247*, 510. (b) Maggini, M.; Guldi, D. M.; Mondini, S.; Scorrano, G.; Paolucci, F.; Ceroni, P.; Roffia, S. *Chem. Euro. J.* **1998**, *4*, 1992. (c) Guldi, D. M.; Garscia, G. T.; Mattay, J. *J. Phys. Chem. A* **1998**, *102*, 9679. (d) Polese, A.; Mondini, S.; Bianco, A.; Toniolo, C.; Scorrano, G.; Guldi, D. M.; Maggini, M. *J. Am. Chem. Soc.* **1999**, *121*, 3446. (e) Guldi, D. M. *Chem. Commun.* **2000**, 321.

(9) (a) Allemand, P. M.; Koch, A.; Wudl, F.; Rubin, Y.; Diederich, F.; Alvarez, M. M.; Anz, S. J.; Whetten, R. L. *J. Am. Chem. Soc.* **1991**, *113*, 1050. (b) Dubois, D.; Kadish, K. M.; Flanagan, S.; Haufler, R. E.; Chibante, L. P. F.; Wilson, L. J. *J. Am. Chem. Soc.* **1991**, *113*, 4364.

(10) (a) Bobrowski, K.; Das, P. K. *J. Phys. Chem.* **1985**, *89*, 5079. (b) Bobrowski, K.; Das, P. K. *J. Phys. Chem.* **1987**, *91*, 1210. (c) Edge, R.; Land, E. J.; McGarvey, D.; Mulroy, L.; Truscott, T. G. *J. Am. Chem. Soc.* **1998**, *120*, 4087.

(11) (a) Sasaki, Y.; Konishi, T.; Yamazaki, M.; Fujitsuka, M.; Ito, O. *Phys. Chem. Chem. Phys.* **1999**, *1*, 4555. (b) Fujitsuka, M.; Luo, C.; Ito, O.; Murata, Y.; Komatsu, K. *J. Phys. Chem. A* **1999**, *103*, 7155. (c) Sasaki, Y.; Fujitsuka, M.; Watanabe, A.; Ito, O. *J. Chem. Soc., Faraday Trans.* **1997**, *93*, 4275. (d) Nojiri, T.; Alam, M. M.; Konami, H.; Watanabe, A.; Ito, O. *J. Phys. Chem. A* **1997**, *101*, 7943. (e) Nojiri, T.; Watanabe, A.; Ito, O. *J. Phys. Chem. A* **1998**, *102*, 5215. (f) Alam, M. M.; Sato, M.; Watanabe, A.; Akasaka, T.; Ito, O. *J. Phys. Chem. A* **1998**, *102*, 7447. (g) Luo, C.; Fujitsuka, M.; Huang, C. H.; Ito, O. *J. Phys. Chem. A* **1998**, *102*, 8716. (h) El-Kemary, M.; Fujitsuka, M.; Ito, O. *J. Phys. Chem. A* **1999**, *103*, 1329.

(12) Luo, C.; Fujitsuka, M.; Watanabe, A.; Ito, O.; Gan, L.; Huang, Y.; Huang, C. H. *J. Chem. Soc., Faraday Trans.* **1998**, *84*, 527.

(13) Murov, S. L.; Carmichael, I.; Hug, G. L. *Handbook of Photochemistry, 2nd ed.*; Marcel Dekker: New York, 1993.

(14) Hung, R. R.; Grabowski, J. J. *J. Phys. Chem.* **1991**, *95*, 6073.

(15) Ebbesen, T. W.; Tanigaki, K.; Kuroshima, S. *Chem. Phys. Lett.* **1991**, *181*, 501.

(16) (a) Bensasson, R.; Long, E. A.; Land, E. J. *J. Chem. Soc., Faraday Trans.* **1977**, *73*, 1319. (b) Chantrell, S. J.; McAulifee, C. A.; Munn, R. W.; Pratt, A. C.; Land, E. J. *J. Chem. Soc.* **1976**, 858.

(17) (a) Arbogast, J. W.; Foote, C. S. *J. Am. Chem. Soc.* **1991**, *113*, 8886. (b) Guldi, D. M.; Hungerbuhler, H.; Janata, E.; Asmus, K.-D. *J. Phys. Chem.* **1993**, *97*, 11258. (c) Fraelich, M. R.; Weisman, R. B. *J. Phys. Chem.* **1993**, *97*, 11145.

(18) (a) Fujitsuka, M.; Ito, O.; Imahori, H.; Yamada, K.; Yamada, H.; Sakata, Y. *Chem. Lett.* **1999**, 721. (b) Konishi, T.; Fujitsuka, M.; Ito, O. *Chem. Lett.* **2000**, 202.

(19) (a) Marcus, R. A. *J. Chem. Phys.* **1956**, *24*, 966. (b) Marcus, R. A. *J. Chem. Phys.* **1965**, *43*, 679. (c) Marcus, R. A.; Sutin, N. *Biochim. Biophys. Acta* **1985**, *811*, 265. (d) Levich, V. *Adv. Electrochem. Electrochem. Eng.* **1966**, *4*, 249.

(20) (a) Zeng, Y.; Zeimmt, M. B. *J. Phys. Chem.* **1992**, *96*, 8395. (b) Kroon, J.; Oevering, H.; Verhoeven, J. W.; Warman, J. M.; Oliver, A. M.; Paddon-Row, M. N. *J. Phys. Chem.* **1993**, *97*, 5065.

(21) (a) Marcus, R. A. *Can. J. Chem.* **1959**, *37*, 155. (b) Marcus, R. A. *J. Chem. Phys.* **1965**, *43*, 2654.

(22) Ghosh, H.; Pal, H.; Sapre, A. V.; Mittal, J. P. *J. Am. Chem. Soc.* **1993**, *115*, 11722.